Journal of Micromechanics and Microengineering

Piezoelectric inkjet coating of injection moulded, reservoir-tipped microneedle arrays for transdermal delivery

To cite this article before publication: Conor O'Mahony *et al* 2019 *J. Micromech. Microeng.* in press https://doi.org/10.1088/1361-6439/ab222b

Piezoelectric Inkjet Coating of Injection Moulded, Reservoir-Tipped Microneedle Arrays for Transdermal Delivery

Conor O'Mahony[1,*], Andrea Bocchino[1], Michael J. Haslinger[2], S. Brandstätter[3], Helene Außerhuber[2], Klaudia Schossleitner[4], A. James P. Clover[5], and Daniel Fechtig[2]

[1]Tyndall National Institute, University College Cork, Cork, Ireland.

[2]PROFACTOR GmbH, Steyr-Gleink, Austria.

[3]STRATEC Consumables GmbH, Anif, Austria.

[4]Skin and Endothelium Research Division, Department of Dermatology, Medical University Vienna, Vienna, Austria

[5]Department of Plastic and Reconstructive Surgery, Cork University Hospital, Cork, Ireland.

Email: conor.omahony@tyndall.ie

Abstract. Coated microneedles have significant potential for use in transdermal delivery applications. In this paper, we describe the fabrication of microneedle master templates using microstereolithography techniques and subsequently use a commercial injection moulding process to replicate these microneedles in biocompatible cyclic olefin polymer (COP) materials. Notably, the 475 μm-tall needle designs feature a shallow pit or reservoir at the tip, thereby providing both a target and holder for incoming droplets that are deposited using a piezoelectric inkjet printer. Using this design, no tilting or rotation of the needle array is required during the filling process. In the preliminary tests reported here, the reservoir is filled with a FITC-labelled dye that acts as a model drug, and *ex-vivo* skin tests are used to verify skin penetration, the transfer of this model drug to the skin and to measure the reliability of the needles themselves. To our knowledge, this is the first time that such an inkjet-filled, reservoir-tipped microneedle has been demonstrated.

Keywords - Microneedles, injection moulding, piezoelectric inkjet dispensing, bioMEMS, transdermal drug delivery, microstereolithography

Submitted to *Journal Of Micromechanics and Microengineering*, 14-01-19

Revised 01-05-19

1 Introduction

Patch-based transdermal drug delivery is highly attractive due to its needle-free nature and potential for self-administration, with corresponding benefits in increased patient compliance, reduced clinical time, elimination of needle-stick injuries and sharps waste. However, the outermost layer of the skin poses a formidable barrier to the transdermal delivery of drugs and vaccines. Despite being relatively thin (typically 10-20μm thick), the *stratum corneum* prevents the passage of all but a small number of low molecular weight drugs, currently estimated at fewer than 20 products [1-3] . However, this specialized and constantly renewing layer of cornified and keratin-rich cell bodies is not the only hurdle to overcome. The skin barrier is further fortified by a high number of cell-cell junctions in the epidermal layers beneath [4]. To efficiently deliver drugs across these multiple barriers in the epidermis of mammalian skin new transdermal drug delivery technologies are needed.

Microneedle technologies have been proposed as a potential solution to this issue. Consisting of short, sharp structures generally measuring less than 1 mm in length and provided in arrays of anything up to several thousand per square centimetre, microneedle patches can be used to penetrate the *stratum corneum* and deliver drugs or vaccines to the viable epidermis immediately below in a painless and minimally invasive manner [5, 6].

These arrays can be deployed in four primary delivery mechanisms. Firstly, simple solid microneedles can be used to painlessly perforate the skin before the subsequent application of a topical formulation or patch [7]. Secondly, drugs and vaccines can be infused in small volumes and at low flowrates through hollow microneedles in much the same manner as with conventional hypodermic needles [8]. Thirdly, a number of techniques such as brushing, dipping, inkjet printing or spraying can be used to coat microneedles with a formulation that is dried and later dissolved in the skin [9]. Lastly, dissolvable microneedles (DMNs) are moulded from a biodegradable polymer into which a drug or vaccine is mixed and which dissolves once in contact with the moist epidermal layers beneath the *stratum corneum* [10].

1.1 Low-cost transdermal drug delivery (TDD) device fabrication

Microneedles have traditionally been fabricated using techniques borrowed from the semiconductor industry, such as photolithography, thin-film deposition, wet and dry etching, and wafer dicing [11, 12]. Although precise and in some cases capable of producing complex and ultrasharp devices that integrate additional functionality such as fluidics and electronics, semiconductor-based processing is expensive, often slow, and tends to use materials that may not be accepted as standard in the medical devices industry. Therefore, there is growing interest in the low-cost, rapid fabrication of transdermal

drug delivery systems (TDDS), using a combination of one or more techniques for fabrication, replication and/or functionalization [13]. Micromoulding has attracted wide interest for low-cost microneedle fabrication, using both solid [14] and biodegradable [15] materials. In particular, biodegradable microneedles have the advantage that the drug or vaccine of interest may be mixed with the structural material. This provides a single-step fabrication process and a low-cost delivery route with the potential for relatively high dose loading [16], and significant progress is being made in addressing issues such as polymer processing temperatures, biomechanical strength and long-term stability during storage [17]. Alternative processes that may provide low-temperature fabrication, such as droplet air blowing [18] and drawing lithography [19], are also emerging as candidates for low-cost needle manufacture.

Among more commercially established technologies, injection moulding is commonly used for the manufacture of biomedical components [20, 21], and has been shown to be capable of replicating the small features and sharp tips usually associated with microneedles, in low cost, high-throughput facilities. 3M Corporation have demonstrated transdermal drug delivery using both solid [22-24] and hollow [25] injection moulded microneedles, fabricated from medical-grade, liquid crystalline polymer materials under their Microstructured Transdermal System (MTS) brand. Others have used injection moulding techniques to create microneedles in materials such as polycarbonate, polyethylene terephthalate (PET), cyclic olefin copolymer (COC), and polyoxymethylene [26-29].

3D printing approaches such as two-photon polymerization (2PP), microstereolithography (μSL) or digital light processing (DLP) are also emerging as a new way of making microneedles, and can now achieve very precise geometries [30]. Ultra-sharp polymer microneedles specifically designed to perforate the round window membrane (RWM) of the inner ear with a view to precisely delivering therapeutics across that membrane were fabricated using 2PP [31], achieving a tip radius of 500 nm. 2PP was also employed to fabricate 630 nm-diameter microneedles for use in single call analysis from a drop cast resist material [32], while μSL was used to develop 700 μm tall biodegradable microneedles for chemotherapeutic drug delivery [33]. 3D printing has also been used to fabricate a curved microneedle array for treatment of trigger finger, and to subsequently deliver diclofenac gel using the 'poke and patch' approach [34] .

These low-cost 3D printing approaches can be merged with non-contact coating techniques, particularly piezoelectric inkjet deposition [35, 36], to form fully functional transdermal drug delivery patches. The team at University of North Carolina and North Carolina State University, have combined μSL and elastomeric vacuum casting to create microneedles from Gantrez polymers, which were then coated with various formulations using piezoelectric printing [37-39]. Later, that group used a combination of injection moulding, drawing lithography and piezoelectric printing to demonstrate poly(glycolic) acid microneedles that were coated with itraconazole and voriconazole formulations [40, 41]. In all cases, deposition was facilitated by carefully arranging the needles so that

a flat face of the needle was positioned at 90° to the incoming droplet path, and in [41], loading was maximised by rotating the needle midway through the process in order to coat both sides. In [42], μSL printing and inkjet disposition were combined for applications in insulin delivery.

Clearly, in studies performed to date, multiple coating steps or careful positioning of the microneedle array substrate is required in order to obtain sufficiently high dose loading. An alternative method of increasing dose loading, without using substrate orientation or multiple deposition passes, could be by modifying the structure of the microneedle tip itself to receive and to hold larger volumes of formulation. In this paper, we therefore describe the fabrication of microneedle master templates using μSL techniques and show that it is possible to use a commercial injection moulding process to replicate these microneedles in cyclic olefin polymers (COPs), with shape and sharpness approaching that of the original master template. Notably, the microneedles have been designed to incorporate a shallow pit or reservoir at the tip, thereby providing both a target and holder for incoming droplets that are deposited using a piezoelectric inkjet printer. This reservoir retains the formulation close to the tip, and also has the potential to increase loading capacity. In the preliminary tests reported here, the reservoir is filled with a FITC-labelled dye that acts as a model drug, and *ex-vivo* skin tests are used to verify the transfer of this model drug to the skin. In addition, we measure the reliability of the needles themselves. To our knowledge, this is the first time that such a reservoir-tipped microneedle has been demonstrated.

2 Experimental Details

2.1 Microneedle master – design and fabrication

Microneedle master templates were produced using microstereolithography (μSL), i.e the spatially controlled solidification of a liquid resin by direct ultraviolet photo-polymerization in a series of layers. The microneedles were designed as 475 μm tall, cone-like structures with a sidewall angle of 73°, at a pitch of 1.4 mm, and incorporating a 180 μm deep reservoir (volume approximately 59 pL) near the tip, figure 1. This bevel-like, offset design positions the drug cargo close to the tip, whilst retaining the tip itself for better skin penetration and needle reliability.

Needles were printed using a custom-built μSLA system using a 375 nm UV-laser diode and a scanning galvanometer mirror to solidify a UV-curing adhesive (07A22X-8, Sony CID Corp., Tokyo). First, a square base for the arrays was printed using 4 x 100 μm thick layers. Next, 5 μm thick layers were used to create the lower body of the needle, while the layer thickness was reduced to 2 μm for the last 15 layers. This smaller step height results in increased accuracy and tip sharpness. Arrays of 5 x 5 needles were produced, and the printing time for one array was roughly 5 hours, depending on the final resolution and chosen layer thickness.

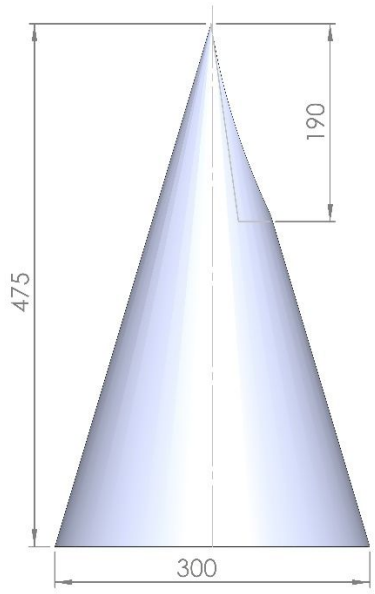

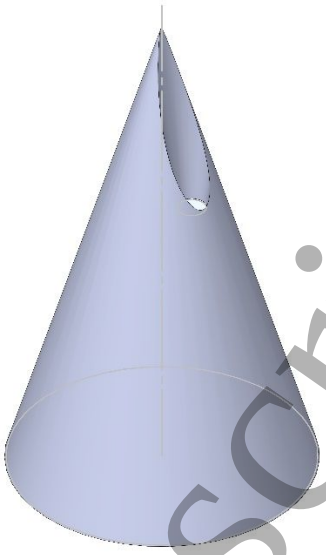

Figure 1. CAD drawing of the microneedle master design.

2.2 Injection Moulding

Using these templates, arrays of sharp polymer microneedle structures were then manufactured at STRATEC Consumables GmbH (Anif, Austria), using a proprietary replication process based on their former CD/DVD production equipment. This involved mounting a customized insert on an existing CD mould, and using an isothermal injection moulding process without compression. A Sumitomo Disc 40E Disc Molding Subsystem (Sumitomo SHI Demag Plastics Machinery North America, Inc., OH, USA) was used for moulding; the mould temperature was 80°C and the clamping pressure set at 25 tons, figure 2. The material was Zeonor 1020R cyclic olefin polymer (Zeon Europe GmbH, Dusseldorf, Germany), which we have already shown to be biocompatible according to ISO 10993-5 and USP 87 standards [43], and the process resulted in easy de-moulding as well as sharp needle tips. A milling procedure was then used to partially isolate each electrode from the frame, leaving the array lightly tethered on two thin supports for subsequent easy removal.

Figure 2. Sumitomo Disc 40E Disc Moulding Subsystem [44].

2.3 Piezoelectric dispensing

The injection moulded needles were then filled using a Dimatix DMP 2800 drop-on-demand inkjet printer (FujiFilm Dimatix, Santa Clara, CA). An actuation pulse of amplitude 15 V and duration of 11.5 µs, and a maximum jetting frequency of 5000 Hz was used. Nominal drop volume was 10pL and the escape velocity of the droplets was between 2-8 m/s.

The ink was a mixture of 5 wt % fluorescein isothiocyanate (FITC) dye for imaging purposes, 22 wt % water and a 73 wt % mixture of volatile solvents. The dry mass of one drop (FTIC) was 0.536 ng per drop. The ink temperature was set to 50 °C, and the printbed was heated to 30 °C. Ambient laboratory conditions (20 °C and relative humidity of 50 %) prevailed. Loaded needles were then dried at 100 °C for 30 minutes.

For these initial tests and to aid with subsequent visualisation of the dye transfer to skin, just one column of each array (i.e 5 x 1 needles) was loaded. Initially the array was aligned with one axis of the printer, and the coordinates of the first needle in the target row were selected using the printhead camera and Dimatix internal software. Subsequent needles were coated by moving the nozzle along the row, in steps equal to the microneedle pitch, starting from the location of this first needle. A variety of deposition settings and skin insertion times were used as specified in Table 1 below.

2.4 Skin preparation and array applications

Following protocols approved by the Clinical Research Ethics Committee of the Cork Teaching Hospitals (CREC), human skin was excised following plastic surgical operations and stored at -80 °C until needed. It was then defrosted, trimmed of excess fat, cut into squares of approximately 3 cm x 3 cm, and mounted on an artificial tissue substrate (Wound Closure Pad, Limbs & Things, Bristol, UK) to mimic the mechanical properties of underlying tissue.

Spring-loaded applicators are often used to apply microneedle devices to the skin in a consistent manner [45]. In this case, a custom-built applicator was used to ensure repeatable and reliable skin penetration. This applicator uses a spring constant of 274 N/m, and generated impact energy of (0.4 +/- 0.01) J/cm^2.

Methylene blue staining is a technique routinely used to assess microneedle penetration [46], and was also used here to confirm skin breach. During this procedure, uncoated arrays (i.e. with empty tip reservoirs) were applied to the skin with the applicator and left in place for 20 minutes. After removal, the impact area was stained with a 1% solution (w/vol) of methylene blue (Sigma-Aldrich, Dublin, Ireland) for 90 minutes. Excess dye was removed with tissue, the skin was cleaned with water and 70% ethanol, before being tape stripped ten times (9040 Paper Tape, 3M Corp., St Paul, MN) in order to ensure than any remaining dye was present under the stratum corneum and not on its surface.

To test the fluorescent dye-loaded microneedle arrays, the applicator maintained a force of (5.90 +/- 0.54) N on the needle array for a specific time after impact. Six arrays were tested at varying insertion times, see Table 1.

Array Number	# drops	Nominal Volume (pL)	Total Dry Mass (ng)	Insertion Time (min)
1	2	20	1,072	10
2	4	40	2,144	10
3	4	40	2,144	5
4	6	60	3,216	5
5	6	60	3,216	1
6	8	80	4,288	1

Table 1. Needle loading parameters and skin insertion times for each sample type.

2.5 Inspection and classification

Optical microscope images of the methylene blue-stained impact area after insertion and skin washing/stripping were recorded using a digital camera. A thorough inspection of the fluorescent dye-loaded needles was also performed. Each of the 6 injection moulded arrays featured 21 needles – a total of 126 needles. Of these, one column (five needles) on each array was filled. Each needle, whether filled or not, was individually inspected both before and after skin insertion, from a variety of angles and orientations, using microscopes including stereozoom (SZX12, Olympus Corp., Tokyo, Japan), digital (VHX-200, Keyence Ltd., Milton Keynes, UK) and fluorescent (Olympus BX51). The purpose of this exercise was to visually confirm delivery of the dye and to assess any damage that occurred during the insertion process.

Following application to *ex-vivo* tissue as outlined above, fluorescent microscopy was used to examine the transfer of material from filled needles to skin. Pictures of the surface of the skin were taken with the fluorescent microscope at exposure times (ETs) of 50 ms, 100 ms and 200 ms.

Finally, the skin samples were cut using a scalpel along the line of the holes left by the loaded needles. Images of the cross section of the skin were taken with the fluorescent microscope to assess the diffusion of the dye underneath the stratum corneum.

In order to quantify the intensity of the fluorescence as a function of array insertion time, an image analysis was performed using the software ImageJ [47]. A region of interest (ROI) was defined by firstly selecting an initial pixel at the boundary of the fluorescent area, and then using the software's 'Wand' tool to identify a contiguous area based on the condition that all the boundary pixel values

must be in the range *initial pixel value* ± *tolerance*, where the tolerance value was set to 22 and kept constant for each image analysis.

To remove the influence of the background signal, the mean intensity per pixel of the region outside of the ROI was calculated for each image, and subtracted from each pixel within the ROI. The total intensity was calculated by summing this net fluorescence per pixel over all pixels within the ROI.

3 Results and Discussion

3.1 Microneedle fabrication using μSL and injection moulding

Images of the μSL master structure and injection-moulded needle array are illustrated in figure 3. Note the milled slot and tethers linking the array to the support frame.

(a)

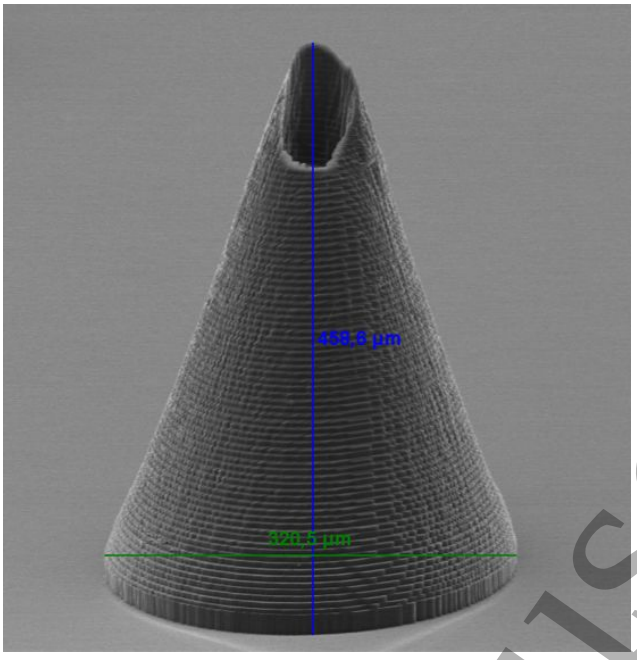

(b)

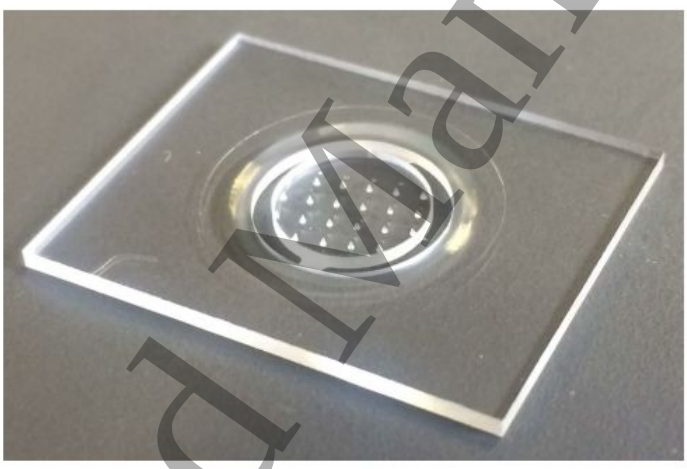

(c)

Figure 3. (a) SEM image of μSL master structure, (b) SEM of injection moulded microneedle, and (c) injection moulded array prior to removal from support frame.

3.2 Filling of needle reservoirs

Background fluorescence from the epoxy material itself prevented a thorough analysis of the polymer microneedle coating using fluorescence microscopy, and so droplet location and consistency was assessed using optical microscopy, figure 4. In general all of the incoming material was positioned in the reservoir and little or no splashing was observed on or around the needle.

Figure 4. Left: example of reservoir-tipped microneedles after the filling procedure. Right: Top-down perspective of filled microneedles.

3.3 Skin Penetration and Delivery

Penetration markings remaining after the staining procedure described in Section 2.4 are shown in figure 5.

Figure 5. Ex-vivo skin sample stained with methylene blue dye following microneedle array insertion. The needle pitch is 1.4 mm.

Methylene blue is hydrophilic with a low molecular weight, and the intact, hydrophobic stratum corneum cannot take up the stain. Once the stratum corneum barrier is disrupted, the dye diffuses through the newly created pores to the underlying epidermis, where it binds to the tissue due to its high affinity for proteins. Therefore, the presence of blue markings after microneedle application is generally regarded as definitive proof of successful insertion. Note that 19 marks are present, while

there are 21 needles on the array, and a closer inspection revealed that two needles on the right-hand side of the array were damaged during handling, resulting in no penetration at these locations.

To establish if the fluorescent dye was delivered inside the skin, analysis of both the microneedle arrays and skin samples was performed as outlined in Section 2.5. Figure 6 illustrates the needle already shown in figure 4 after skin insertion for ten minutes.

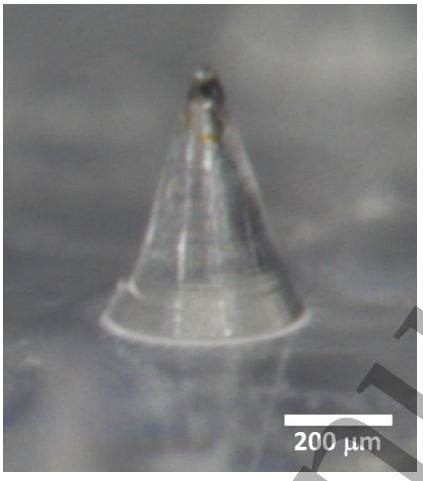

Figure 6. Microneedle of figure 3 (left) shown after skin insertion.

The dye almost completely disappeared from the tip of the microneedle, indicating that it was transferred to the skin. Further evidence of transdermal delivery is evident from the fluorescent photos of the skin samples. As shown in figures 7 and 8, the points where the skin was pierced by the needles are clearly visible and the fluorescent dye has diffused beneath the stratum corneum.

Figure 7. Cross-section of skin sample. The point of needle insertion and diffusion of dye beneath the surface is clearly visible.

To quantify the dye delivery process as outlined in Section 2.5, the background contribution was removed and the value of the fluorescence recalculated for the entire row of dye-loaded needles, figure 8. Exposure time for all of this analysis was 50 ms (as longer exposures tended to exhibit

saturation) and the resultant intensity data is shown in figure 9. Two independent variables are present, i.e. droplet quantity and skin insertion time. In general, the results are as expected, i.e. increasing either the number of droplets or the skin insertion time results in an increase in fluorescent intensity.

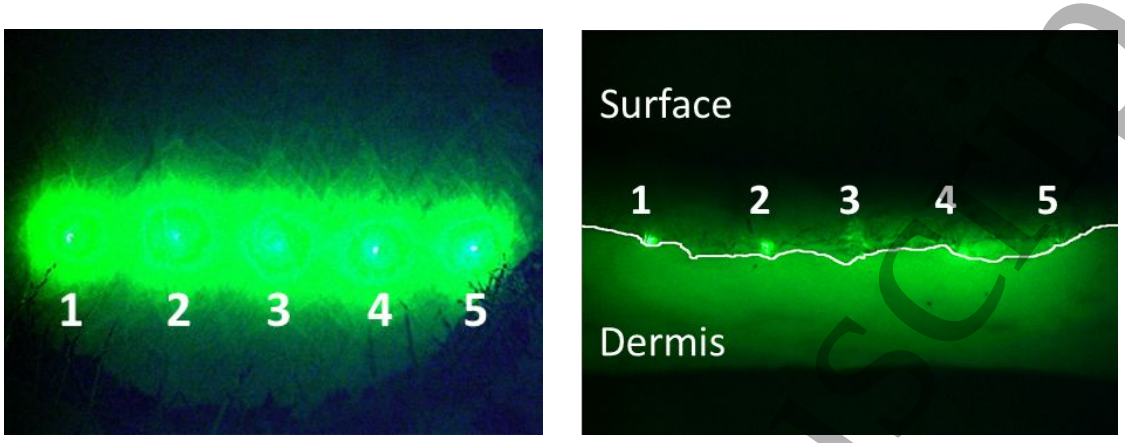

Figure 8. Delivery to skin. Left: En-face image. Right: cross-section of the same skin sample; the boundary between skin surface and underlying tissue is marked. Images taken after ten minutes insertion at 50 ms exposure time. The needle pitch is 1.4 mm.

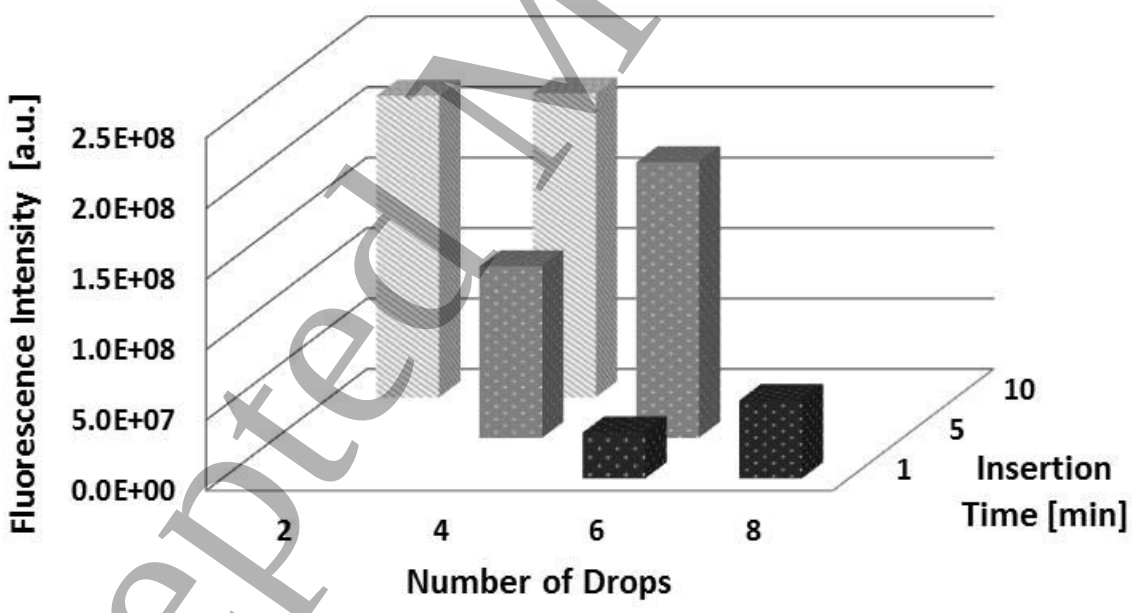

Figure 9. Fluorescence intensity as a function of skin insertion time and needle loading.

The only exception to this trend is for ten-minute insertion times, where the fluorescence intensities are much higher than for one- or five-minute insertion times, but do not vary significantly as a

function of loading volume. This may be caused by the skin becoming saturated after that period, meaning that additional dye delivery does not alter the fluorescence readings.

This is the first demonstration of an injection-moulded, reservoir-tipped microneedle. However, this preliminary proof-of-concept work is limited in scope and additional tests of larger sample sets are required in order to draw definitive statistical conclusions. Secondly, while useful for initial device validation during process development, this fluorescence method is somewhat limited due to its projection of a three-dimensional diffusion pattern onto a two-dimensional image. Future development will require more accurate quantification of drug loading and release profiles through the use of assays such as HPLC analysis and *in-vitro*/*in-vivo* models. However, these results verify transdermal delivery of the model drug from reservoir-tipped needles. Delivery trends are as expected, and show that this novel needle design offers a promising method of transdermal delivery.

3.4 Reliability

During post-insertion inspection, it was noted that a significant number of needles suffered minor tip damage during the skin delivery tests. One array was damaged after removal due to manual handling, and, of the other five arrays that competed a full inspection, 33% of all needles indicated some degree of tip damage. This was always confined to the tip region and no major structural failures of the body of the microneedles were observed. Needle tips seemed to be flattened or crushed, i.e. no breakage or brittle fracture was seen. It is therefore unlikely that any material remained in the skin after use, and, as these are single-use devices, this tip blunting should not pose a major issue. It is nevertheless undesirable and other polymers and/or tip designs should be investigated.

4 Conclusion

This paper has shown that two low-cost techniques – injection moulding and inkjet printing – may be combined to produce coated microneedles for transdermal drug and vaccine delivery. Initially, μSL was used to produce 475 μm tall microneedles, which featured a flat-bottomed pit or reservoir located close to the needle tip. This reservoir increases loading capacity and removes the need to tilt samples in order to present a flat surface to the incoming droplet.

These designs were then replicated at a commercial injection-moulding facility, using a modified process based on former CD/DVD production equipment. An inkjet printer was used to deposit a model drug (FITC) into the reservoir, and needle arrays were inserted into *ex-vivo* human skin using an applicator. Subsequent fluorescence analysis showed the results were largely in line with expectations, i.e. intensity increased with needle loading and skin insertion time. This work shows that it is feasible to rapidly produce large quantities of coated microneedle arrays, using automated processes, in medical-grade material and at low cost.

Acknowledgement

This work was financially supported by the BMVIT - Bundesministerium für Verkehr, Innovation und Technologie (Austria) and was conducted in the framework of the program "Production of the future" (MicroNeedle, Grant 853482). This work has also been partially supported by the Science Foundation Ireland INSIGHT Centre, by Enterprise Ireland (CF/2012/2339), and by the Higher Education Authority under the Programme for Research in Third-Level Institutions.

References

[1] A. C. Watkinson, "A commentary on transdermal drug delivery systems in clinical trials," *Journal of Pharmaceutical Sciences* **102**, pp. 3082-3088, 2013.

[2] M. R. Prausnitz and R. Langer, "Transdermal drug delivery," *Nature biotechnology* **26**, pp. 1261-8, 2008.

[3] A. Morteza, S. Sahar, N. B. J., and S. Metin, "Recent Advances in Wearable Transdermal Delivery Systems," *Advanced Materials* **30**, p. 1704530, 2018.

[4] C. M. Niessen, "Tight junctions/adherens junctions: basic structure and function," *Journal of Investigative Dermatology* **127**, pp. 2525-2532, 2007.

[5] M. R. Prausnitz, "Engineering microneedle patches for vaccination and drug delivery to skin," *Annual review of chemical and biomolecular engineering* **8**, pp. 177-200, 2017.

[6] K. Ita, "Transdermal Delivery of Drugs with Microneedles—Potential and Challenges," *Pharmaceutics* **7**, p. 90, 2015.

[7] J. B. Carey, F. E. Pearson, A. Vrdoljak, M. G. McGrath, A. M. Crean, P. T. Walsh*, et al.*, "Microneedle array design determines the induction of protective memory CD8+ T cell responses induced by a recombinant live malaria vaccine in mice," *PLoS One* **6**, p. e22442, 2011.

[8] M. Dul, M. Stefanidou, P. Porta, J. Serve, C. O'Mahony, B. Malissen*, et al.*, "Hydrodynamic gene delivery in human skin using a hollow microneedle device," *Journal of Controlled Release* **265**, pp. 120-131, 2017.

[9] R. Haj-Ahmad, H. Khan, M. S. Arshad, M. Rasekh, A. Hussain, S. Walsh*, et al.*, "Microneedle Coating Techniques for Transdermal Drug Delivery," *Pharmaceutics* **7**, pp. 486-502, 2015.

[10] M. Leone, J. Mönkäre, J. A. Bouwstra, and G. Kersten, "Dissolving Microneedle Patches for Dermal Vaccination," *Pharmaceutical research* **34**, pp. 2223-2240, 2017.

[11] S. Henry, D. V. McAllister, M. G. Allen, and M. R. Prausnitz, "Microfabricated microneedles: a novel approach to transdermal drug delivery," *Journal of pharmaceutical sciences* **87**, pp. 922-925, 1998.

[12] C. O'Mahony, "Structural characterization and in-vivo reliability evaluation of silicon microneedles," *Biomedical microdevices* **16**, pp. 333-343, 2014.

[13] S. Indermun, R. Luttge, Y. E. Choonara, P. Kumar, L. C. Du Toit, G. Modi*, et al.*, "Current advances in the fabrication of microneedles for transdermal delivery," *Journal of controlled release* **185**, pp. 130-138, 2014.

[14] C. O'Mahony, K. Grygoryev, A. Ciarlone, G. Giannoni, A. Kenthao, and P. Galvin, "Design, fabrication and skin-electrode contact analysis of polymer microneedle-

based ECG electrodes," *Journal of Micromechanics and Microengineering* **26**, p. 084005, 2016.

[15] E. A. Allen, C. O'Mahony, M. Cronin, T. O'Mahony, A. C. Moore, and A. M. Crean, "Dissolvable microneedle fabrication using piezoelectric dispensing technology," *International journal of pharmaceutics* **500**, pp. 1-10, 2016.

[16] X. Hong, L. Wei, F. Wu, Z. Wu, L. Chen, Z. Liu*, et al.*, "Dissolving and biodegradable microneedle technologies for transdermal sustained delivery of drug and vaccine," *Drug design, development and therapy* **7**, p. 945, 2013.

[17] K. Ita, "Dissolving microneedles for transdermal drug delivery: Advances and challenges," *Biomedicine & Pharmacotherapy* **93**, pp. 1116-1127, 2017.

[18] J. D. Kim, M. Kim, H. Yang, K. Lee, and H. Jung, "Droplet-born air blowing: novel dissolving microneedle fabrication," *Journal of controlled release* **170**, pp. 430-436, 2013.

[19] K. Lee and H. Jung, "Drawing lithography for microneedles: a review of fundamentals and biomedical applications," *Biomaterials* **33**, pp. 7309-7326, 2012.

[20] L. Zema, G. Loreti, A. Melocchi, A. Maroni, and A. Gazzaniga, "Injection Molding and its application to drug delivery," *Journal of Controlled Release* **159**, pp. 324-331, 2012.

[21] U. M. Attia, S. Marson, and J. R. Alcock, "Micro-injection moulding of polymer microfluidic devices," *Microfluidics and Nanofluidics* **7**, p. 1, 2009.

[22] D. Duan, C. Moeckly, J. Gysbers, C. Novak, G. Prochnow, K. Siebenaler*, et al.*, "Enhanced delivery of topically-applied formulations following skin pre-treatment with a hand-applied, plastic microneedle array," *Current drug delivery* **8**, pp. 557-65, 2011.

[23] S. Kommareddy, B. C. Baudner, A. Bonificio, S. Gallorini, G. Palladino, A. S. Determan*, et al.*, "Influenza subunit vaccine coated microneedle patches elicit comparable immune responses to intramuscular injection in guinea pigs," *Vaccine* **31**, pp. 3435-41, 2013.

[24] Y. Zhang, K. Brown, K. Siebenaler, A. Determan, D. Dohmeier, and K. Hansen, "Development of Lidocaine-Coated Microneedle Product for Rapid, Safe, and Prolonged Local Analgesic Action," *Pharmaceutical research* **29**, pp. 170-177, 2012.

[25] S. A. Burton, C.-Y. Ng, R. Simmers, C. Moeckly, D. Brandwein, T. Gilbert*, et al.*, "Rapid intradermal delivery of liquid formulations using a hollow microstructured array," *Pharmaceutical research* **28**, pp. 31-40, 2011.

[26] K. B. Mirza, C. Zuliani, B. Hou, F. S. Ng, N. S. Peters, and C. Toumazou, "Injection moulded microneedle sensor for real-time wireless pH monitoring," in *2017 39th Annual International Conference of the IEEE Engineering in Medicine and Biology Society (EMBC)*, 2017, pp. 189-192.

[27] K. Nair, B. Whiteside, C. Grant, R. Patel, C. Tuinea-Bobe, K. Norris*, et al.*, "Investigation of Plasma Treatment on Micro-Injection Moulded Microneedle for Drug Delivery," *Pharmaceutics* **7**, pp. 471-85, 2015.

[28] F. Sammoura, J. Kang, Y.-M. Heo, T. Jung, and L. Lin, "Polymeric microneedle fabrication using a microinjection molding technique," *Microsystem Technologies* **13**, pp. 517-522, 2007.

[29] K. Yung, Y. Xu, C. Kang, H. Liu, K. Tam, S. Ko*, et al.*, "Sharp tipped plastic hollow microneedle array by microinjection moulding," *Journal of Micromechanics and microengineering* **22**, p. 015016, 2011.

[30] S. H. Lim, H. Kathuria, J. J. Y. Tan, and L. Kang, "3D printed drug delivery and testing systems — a passing fad or the future?," *Advanced Drug Delivery Reviews* 2018.

[31] A. Aksit, D. N. Arteaga, M. Arriaga, X. Wang, H. Watanabe, K. E. Kasza*, et al.*, "In-vitro perforation of the round window membrane via direct 3-D printed microneedles," *Biomedical Microdevices* **20**, p. 47, 2018.

[32] K. Mincho, P. Jose Efrain, I. Yurii, B. Andrea, L. Carlo, and K. Jürgen, "Biocompatible 3D printed magnetic micro needles," *Biomedical Physics & Engineering Express* **3**, p. 025005, 2017.

[33] Y. Lu, S. N. Mantha, D. C. Crowder, S. Chinchilla, K. N. Shah, Y. H. Yun*, et al.*, "Microstereolithography and characterization of poly (propylene fumarate)-based drug-loaded microneedle arrays," *Biofabrication* **7**, p. 045001, 2015.

[34] S. H. Lim, J. Y. Ng, and L. Kang, "Three-dimensional printing of a microneedle array on personalized curved surfaces for dual-pronged treatment of trigger finger," *Biofabrication* **9**, p. 015010, 2017.

[35] C. O'Mahony, L. Hilliard, T. Kosch, A. Bocchino, E. Sulas, A. Kenthao*, et al.*, "Accuracy and feasibility of piezoelectric inkjet coating technology for applications in microneedle-based transdermal delivery," *Microelectronic Engineering* **172**, pp. 19-25, 2017.

[36] M. J. Uddin, N. Scoutaris, P. Klepetsanis, B. Chowdhry, M. R. Prausnitz, and D. Douroumis, "Inkjet printing of transdermal microneedles for the delivery of anticancer agents," *International Journal of Pharmaceutics* **494**, pp. 593-602, 2015.

[37] R. D. Boehm, P. R. Miller, S. L. Hayes, N. A. Monteiro-Riviere, and R. J. Narayan, "Modification of microneedles using inkjet printing," *AIP Advances* **1**, p. 022139, 2011.

[38] R. D. Boehm, P. R. Miller, W. A. Schell, J. R. Perfect, and R. J. Narayan, "Inkjet Printing of Amphotericin B onto Biodegradable Microneedles Using Piezoelectric Inkjet Printing," *JOM* **65**, pp. 525-533, 2013.

[39] R. D. Boehm, P. R. Miller, J. Daniels, S. Stafslien, and R. J. Narayan, "Inkjet printing for pharmaceutical applications," *Materials Today* **17**, pp. 247-252, 2014.

[40] R. D. Boehm, J. Daniels, S. Stafslien, A. Nasir, J. Lefebvre, and R. J. Narayan, "Polyglycolic acid microneedles modified with inkjet-deposited antifungal coatings," *Biointerphases* **10**, p. 011004, 2015.

[41] R. D. Boehm, P. Jaipan, S. A. Skoog, S. Stafslien, L. VanderWal, and R. J. Narayan, "Inkjet deposition of itraconazole onto poly (glycolic acid) microneedle arrays," *Biointerphases* **11**, p. 011008, 2016.

[42] C. P. P. Pere, S. N. Economidou, G. Lall, C. Ziraud, J. S. Boateng, B. D. Alexander*, et al.*, "3D printed microneedles for insulin skin delivery," *International Journal of Pharmaceutics* **544**, pp. 425-432, 2018.

[43] K. Schossleitner, C. O'Mahony, S. Brandstatter, M. J. Haslinger, S. Demuth, D. Fechtig*, et al.*, "Differences in biocompatibility of microneedles from cyclic olefin polymers with human endothelial and epithelial skin cells," *Journal of biomedical materials research. Part A* **107**, pp. 505-512, 2019.

[44] (2019, 15 April). *SD40E Disc Molding Subsystem*. Available: http://www.sumitomo-shi-demag.us/sd40emain.html

[45] T. RR Singh, N. J Dunne, E. Cunningham, and R. F Donnelly, "Review of patents on microneedle applicators," *Recent Patents on Drug Delivery & Formulation* **5**, pp. 11-23, 2011.

[46] G. Li, A. Badkar, S. Nema, C. S. Kolli, and A. K. Banga, "In vitro transdermal delivery of therapeutic antibodies using maltose microneedles," *International journal of pharmaceutics* **368**, pp. 109-115, 2009.

[47] C. T. Rueden, J. Schindelin, M. C. Hiner, B. E. DeZonia, A. E. Walter, E. T. Arena, *et al.*, "ImageJ2: ImageJ for the next generation of scientific image data," *BMC Bioinformatics* **18**, p. 529, 2017.